

A techno-economic survey on high- to low-temperature waste heat recovery cycles for UK glass sector

Narges H. Mokarram, Zhibin Yu & Muhammad Imran

To cite this article: Narges H. Mokarram, Zhibin Yu & Muhammad Imran (2023): A techno-economic survey on high- to low-temperature waste heat recovery cycles for UK glass sector, International Journal of Green Energy, DOI: [10.1080/15435075.2023.2197993](https://doi.org/10.1080/15435075.2023.2197993)

To link to this article: <https://doi.org/10.1080/15435075.2023.2197993>



© 2023 The Author(s). Published with license by Taylor & Francis Group, LLC.



Published online: 09 Apr 2023.



Submit your article to this journal [↗](#)



Article views: 178



View related articles [↗](#)



View Crossmark data [↗](#)

A techno-economic survey on high- to low-temperature waste heat recovery cycles for UK glass sector

Narges H. Mokarram^a, Zhibin Yu^a, and Muhammad Imran^b

^aDivision of systems, power and energy, University of Glasgow, Glasgow, UK; ^bCollege of Engineering and Physical Sciences, Department of Mechanical, Biomedical and Design Engineering, Aston University, Birmingham, UK

ABSTRACT

Three heat recovery cycles are studied to recover the waste heat from the exhaust gas outlet of a glass-melting furnace. To determine the viability and potential dangers based on techno-economic aspects, three fundamental recovery cycles for the exhaust gas from UK glass melting furnaces are examined. The parametric thermodynamic and techno-economic study reveals the effects of the key parameters: The condenser temperature of the ORC cycle, the pressure ratio of the $s\text{CO}_2$ cycle, and the flash pressure of the Kalina cycle. Three thermodynamic parameters (Power production, energy, and exergy efficiency), as well as five techno-economic parameters (LCOE, NPV, PP, IRR, and MOIC), have been studied with varying key factors. The results showed that ORC is the best possible option for low-temperature waste exhaust gases as it is not as expensive as other ones, while super-critical CO_2 has the highest power production to produce power from high-temperature waste heat sources. Even though ORC's payback period is 10% longer than $s\text{CO}_2$'s, Comparing the IRR, NPV, and MOIC of the ORC cycle to those of the $s\text{CO}_2$ cycle, the differences are just 8.3%, 5.3%, and 8.2% lower.

ARTICLE HISTORY

Received 24 December 2022
Accepted 4 February 2023

KEYWORDS

Economic; efficiency; Glass sector; waste heat recovery

1. Introduction

Numerous applications that reject waste heat to the atmosphere in the manufacturing sector operate at a range of temperatures. This leads to two different types of pollution: 1) the flue gases' pollutants (CO_2 , NO_x , SO_x , and HC), which will progressively cause health and environmental catastrophes; 2) Heat rejection also disturbs natural equilibriums because its unfavorable effects manifest as nature's anger in the form of wildfires, storms, forest fires that started on their own, melting ice, etc. Therefore, it is a crucial responsibility for researchers and policymakers to plan and perform the most practical and reliable solutions (Nascimento 2014).

According to data from the US, Germany, and Europe (EU-12), 750 MWe, 500 MWe, and 3000 MWe, respectively, of heat can be recovered through the production of electricity from industrial waste heat (Sovacool et al. 2021). Waste heat recovery has a particularly significant potential in some industries, such as cement, glass, steel, etc. The 0.5 MWe ORC power cycle at the OI (Owens-Illinois manufacturer) Glass container plant in Villotta di Chions, Italy, and the Siemens waste heat recovery sites in Germany, which convert 60% of their waste heat energy to power, are examples of waste heat recovery sites that have already been installed and are in operation in Europe (The European Container Glass Federation-).

Currently, the UK glass industry produces more than 3 Mt of glass annually and plays a crucial role in the supply chain for many of the most significant domestic manufacturing industries, including the food and beverage, construction, renewable energy, and automotive sectors (Glass 2017). Natural gas, the

industry's main energy source, is mostly used in the high-temperature, energy-intensive process of melting glass. The exhaust gas temperature is in the range of 400–500°C, and with recuperators of air-fired furnaces, it even goes up to 700°C or higher. But at oxygen-fired glass melting furnaces, the temperature exceeds 1,100°C (Dolianitis et al. 2016).

According to Figure 1, the UK's enormous glass sector is made up of 10 enterprises spread across 14 locations in England, Scotland, and Northern Ireland. The hot flue gas has lost about a third of the thermal energy that was supplied to the furnaces. Regenerators are being used in 31 of 34 glass manufacturing facilities in the UK to warm the air before it enters the combustion chamber. Another strategy involves using generating power cycles to recover waste heat, which increases system efficiency overall. But recovering the thermal energy from flue gases is limited because it must prevent corrosion at temperatures below the flue gases' acid dew point (Dalton et al. 2019)

The process of glass manufacturing provides a variety of temperature ranges as well as opportunities to recover the possible waste thermal energy. In the first step, the raw material of quartz sand experiences cleaning, calcification, and cracking to reach a finer form with lower impurities. The whole first step process named patch preparation is performed in a range of 15–325°C. The second step is melting the remaining material from the first step in furnaces at a temperature of 1200–1600°C. Then, annealing will be the third step followed by out-gassing and washing as the post-forming step ended up with a temperature range of 100–600°C. Molten glass cannot be used to recover waste heat because the glass melt leaving the melting furnace must meet a certain and predetermined

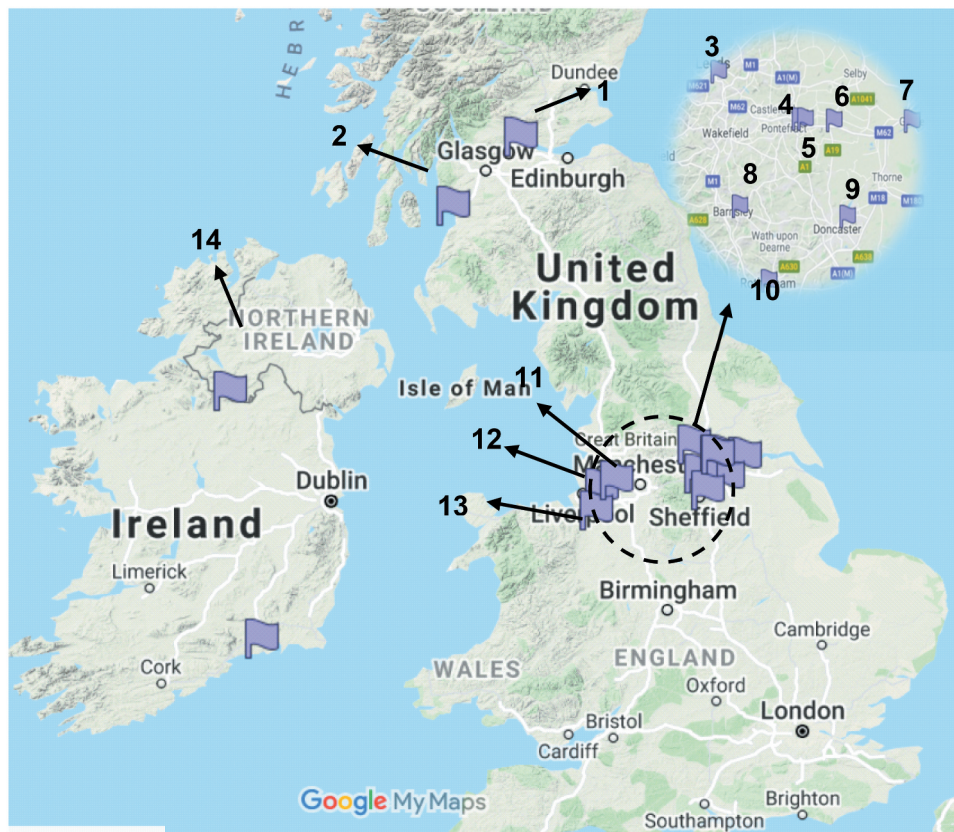


Figure 1. Glass manufacturing sites in England, Scotland and Northern Ireland (Glass Alliance Europe 2022).

temperature profile. It should be noted that only waste heat from the combustion of exhaust gases can theoretically be recovered among all waste heat recovery methods.

However, there are different options to recover the waste heat and increase the efficiency of the glass manufacturing process. Figure 2 shows different thermochemical types of waste heat recovery systems from the exhaust gases of glass melting processes. For each type, the temperature range of the outlet flue gas is referred to. A temperature range of 200–650 is possible to exploit with further plans of recovery systems; however, the minimum temperature of flue gases is limited due to the dew point temperature of flue gases and the possibility of acid corrosion in components.

It is shown that waste heat recovery is one of the most promising methods to overcome climate change. However, the presence of a significant amount of waste heat produced during industrial production looks flirtatious and opportunistic. Waste heat energy is supposed to be among the topmost contributors to greenhouse gas mitigation by 2050. In a waste heat recovery system using a power cycle, the available waste heat is used to power a bottoming cycle turbine and transform thermal energy into electricity. It is significant to note that, depending on the characteristics of each cycle, operating temperature will determine the kind of cycle (Hedin et al. 2013; Philibert 2007).

A variety of power cycles, such as the Stirling cycle, carbon dioxide cycle (CDC), Kalina cycle (KC), organic Rankine cycle (ORC), air bottoming cycle (ABC), and absorption

refrigeration cycle, have been proposed and studied for waste heat recovery (WHR) to increase the efficiency of the systems (Yu et al. 2015)– (Shu et al. 2013)–(Omar. A et al. 2019). In industrial processes, waste heat does exist – some of it avoidable, some of it not. It is not possible to transform unavoidable waste heat into avoidable heat, mostly because of limitations imposed by the second law of thermodynamics and the state of current technologies. There are many heat-recovery cycles that can recover waste heat from flue gas, cooling fluids, and exhaust steam depending on the type of working fluid used as the carrier medium (Brückner et al. 2015).

Three different sub-cycles are common to recover the waste heat in different applications:

Organic Rankine Cycle: ORC. 2-Kalina ammonia-water cycle. 3- Supercritical CO_2 : $s\text{CO}_2$.

In order to generate electricity from a lower-level heat source, such as industrial waste heat, the working fluid is an organic compound with a boiling temperature lower than water (Sovacool et al. 2020). The vaporization of a high-pressure or high temperature working fluid is the basis for both the Organic Rankine Cycle (ORC) and the standard Rankine cycle, often known as the steam power cycle. An evaporator vaporizes a compressed liquid, and the evaporated liquid then expands in the turbine to produce electricity. Following the condenser, the fluid is pumped back to the evaporator after being condensed there. In light of this, an ORC has the same structure and parts as a standard Rankine cycle (Quoilin et al. 2013). The use of low-temperature heat

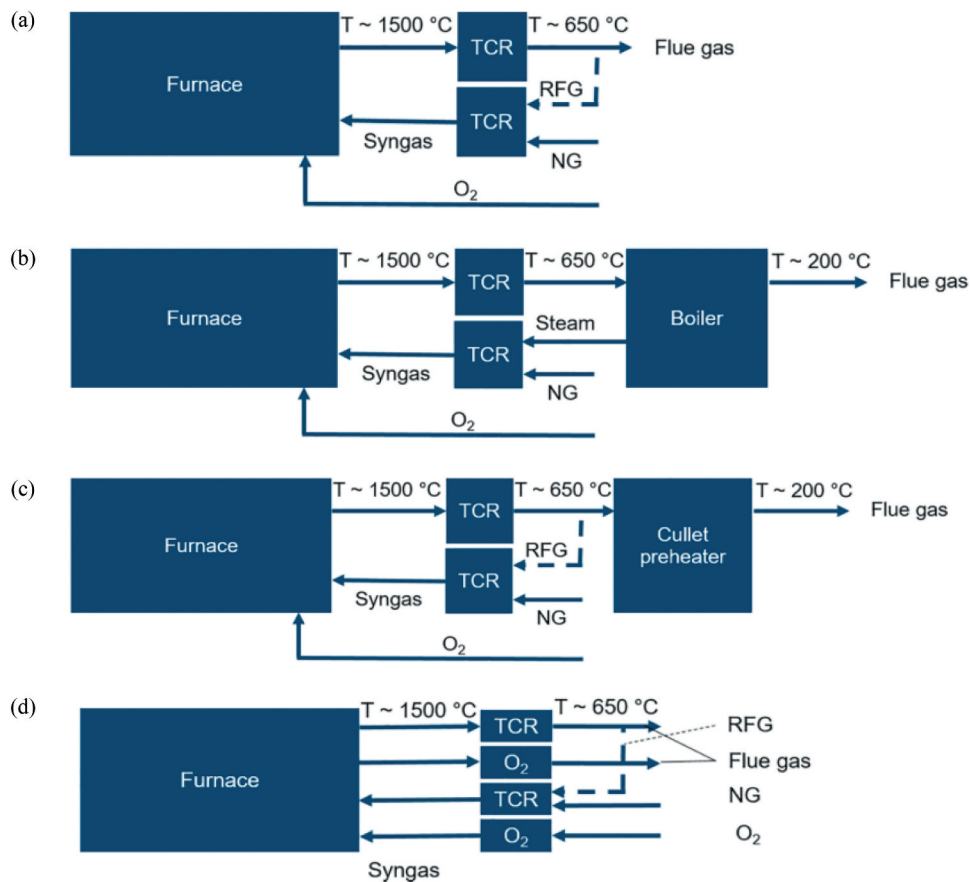


Figure 2. Thermochemical heat recovery processes: (a) Baseline; (b) Baseline +steam boiler; (c) Baseline +cullet preheater; and (d) Baseline +O₂-Regenerator (Zier et al. 2021).

sources by power-producing ORCs has been researched in numerous examples over the past few decades (Larjola 1995; Polytechnic 1998).

Leibowitz and Kalina own the first 3 MW Kalina cycle (KC) patent (Kalina et al. 1988). They demonstrated that, compared to an ORC system with the same peak temperature, a single-pressure KC configuration delivers up to 25% more power. The Kalina cycle is a cutting-edge power cycle that can be used to recover waste heat. The working fluid, a zeotropic mixture of water and ammonia, goes through a cycle in which the concentration of ammonia varies at different state points. The advantage of the Kalina cycle over other cycles is that the ammonia begins to evaporate first during the boiling phase, leaving a mixture with a low concentration and raising the boiling temperature. It describes the non-isothermal process of evaporation and condensation of the mixture of ammonia and water. As a result, the recovery cycle's temperature differential from the exhaust gases is reduced, enabling more effective heat transfer (Omar et al. 2019; Wang, Dai, and Gao 2009).

An evaporator connected to a heat source, such as a waste heat stream, is included in a simplified model of the Kalina cycle along with a turbine, generator, one or two recuperators, condenser, pump, separator, throttle valve, mixer, and other components (Modi 2015).

As the working fluid of the Kalina cycle, the ammonia/water mixture heats up in the evaporator and separates into two phases. The saturated liquid and saturated vapor from the

wet vapor will next be separated in the flash tank. A shift in the liquid and vapor phases of each stream after the tank results in a change in the ammonia concentration in the water solution. The rich blend of saturated vapor enters the turbine to produce electricity. At the regenerator, saturated liquid gains heat and passes through an expansion valve until it reaches condensing pressure. The rich stream is then combined with the turbine outflow in the mixture. The cooling fluid will reject the heat from the turbine's low-pressure vapor when it enters the condenser. The cycle is then continued by pumping the fluid to the regenerator and evaporator (Mokarram and Mosaffa 2018).

The third option is to couple a supercritical CO₂ cycle to extract the wasted heat of the exhaust gas. While conventional power plant cycles produce power from turbines using water or steam as the working fluid, supercritical carbon dioxide (sCO₂) cycles use CO₂ that is in a supercritical state – at a temperature and pressure above its critical point where the liquid and gas phases are not distinguishable. The working fluid is compressed into a compressor and heated by a heat source. Then, the working fluid at high temperature and pressure enters the turbine to be expanded to the low pressure of the cycle, which means to produce power. The outlet flow from the turbine is used to preheat the compressed fluid before entering the condenser (Noaman et al. 2019).

MUSIAŁ et al. (Musiał et al. 2021) calculated the performance of an ORC system, with different working fluids extracted energy from the waste heat of a gas-fired glass

melting furnace. It is assumed that a single-stage axial turbine runs in the system, which leads to producing 300 kW (309 kW for megawatts in the cogenerative mode to 367 kW for toluene in the non-cogenerative mode). The results showed that the efficiency, depending on the working fluid and the working conditions, will be in a range from 14.85% to 16.68%.

Working fluid selection has been carried out by Li et al. (Li and Wang 2016), who also introduce an unique enhanced transcritical CO_2 cycle and two combined designs. A few study examples that use flue gas that has a temperature range of 200°C to 700°C with a minimum temperature of 120°C are looked at. According to the parametric optimization study, the regenerative organic transcritical cycle generates the most power at a source temperature of 500°C , while various optimum working fluids are attained at various heat source temperatures. According to the results, when the source temperature is below 500°C , the Organic Rankine cycle performs well thermodynamically; however, the transcritical cycle marginally generates more power.

The first ORC-based heat recovery system planned by Turboden combined with an Electric Arc Furnace (EAF) with a furnace capacity of 133 t/h and tap-to-tap time of 45 min at Elbestahlwerke Feralpi located at Riesa, Germany (Bause et al. 2014). The recovery system is designed to produce 3 MW of electricity, which is authorized to run since Dec 2013.

According to (Tartière and Astolfi 2017), ORC units produce electricity from industrial thermal energy waste of as much as 376 MW excluding 39 MW of the under-construction units in 2017. Eight of the units were designed for waste heat recovery in the glass sector with 4.7% of the total power capacity installed in ORC systems on industrial plants.

Lecompte et al. (Lecompte et al. 2017) proposed an ORC cycle as a waste heat recovery option from the exhaust gases of an operational 100 MWe electric arc furnace in Belgium. The results show that in an optimized state, a subcritical ORC system will generate 752 kWe electrical output. As a second plan, a combined power generation and heating with a hot water loop ($90\text{--}70^\circ\text{C}$) at the condenser side for heating is considered to produce 521 kWe of electricity (which is 30.7% lower compared to the case without heating) with 4.52 MW of heat generation, which can be utilized on-site for heating space or water or within a heat network. However, to make the system practical, the study needs a comprehensive financial analysis.

Baldi et al. (Baldi and Gabriellii 2015) proposed a new method and performed an exergy analysis to study a waste heat recovery system that is installed to extract the available amount of waste thermal energy. It is revealed that the recovery system will lead to a 4%–16% reduction in fuel consumption depending on the heat source type.

In this research, the waste heat recovery feasibility of the Glass industry using power production cycles will be investigated. The plan in this survey is to investigate the three types of waste heat recovery cycles to use in the UK Glass industry: Organic Rankine cycle (ORC), Kalina cycle, and Supercritical CO_2 cycle to be combined with a flue gas outlet of a Glass Plant site. First, thermodynamic, and then techno-economic analysis will be performed to compare the possible options and discuss the results. The exhaust gas flows out at around $200\text{--}650^\circ\text{C}$,

therefore it will play the role of the hot temperature sources in the considered waste heat recovery cycles in this study.

Finally, the different parameters assumed as the input parameters will be studied. This parametric study helps to find out in which condition it is better to run the system to achieve the highest efficiency and lowest price.

2. Methodology

The composition of the exhaust gas mixture, which is used as the high-temperature source fluid, based on molar fractions is shown in Table 1.

Three different cycles are studied in this research as the waste heat recovery cycles: 1-Organic Rankine Cycle (ORC), 2-Kalina cycle 3-Supercritical CO_2 cycle (sCO_2). The following Figures 3,4,5 show the schematic configurations of the mentioned bottoming cycles.

- Throughout this study, some parameters considered constant such as the operating conditions, which are also listed in Tables 2, 3, and 4.

Table 1. The composition of exhaust gas from a real furnace in a glass manufacturing site (Valenti, Valenti, and Staboli 2019).

| Exhaust gas composition | Value | Unit | Molar Mass (g/mol) |
|-------------------------|--------|---------|--------------------|
| N_2 | 72.46% | mol/mol | 28.013 |
| O_2 | 6.47% | mol/mol | 31.999 |
| CO_2 | 8.75% | mol/mol | 44.010 |
| H_2O | 13.47% | mol/mol | 18.015 |
| Ar | 0.85% | mol/mol | 39.948 |

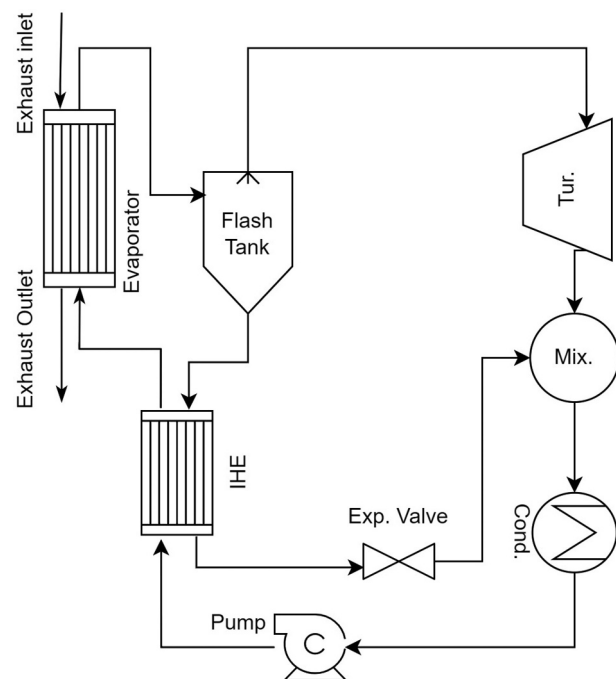


Figure 3. Schematic figure of Kalina cycle as the waste heat recovery system of flue gas outlet from glass sector. The figures in the word file are better than the figures I see here. Some lines are rotated some how. Even some lines turned thicker. So I have changed the figures so the system cannot change them automatically.

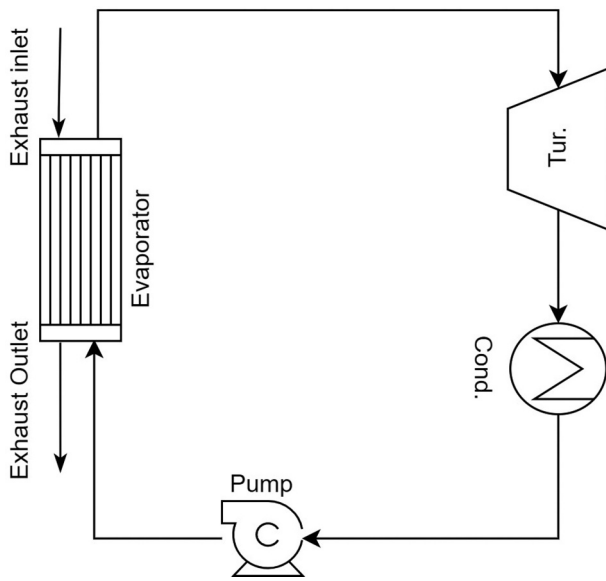


Figure 4. Schematic figure of ORC cycle as the waste heat recovery system of flue gas outlet from Glass sector.

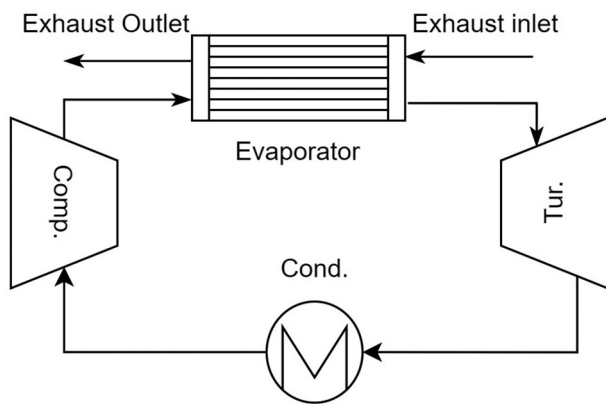


Figure 5. Schematic figure of sCO₂ cycle as the waste heat recovery system of flue gas outlet from glass sector.

- In addition, as the engineering idealization to ease performing the calculations, the authors consider the following fundamental assumptions:
- All cycles' parts function in a steady-state circumstances.
- Without fail, the components and the pipelines that connect them will not experience heat loss and pressure drops.

- The processes have no effect on the streams' kinetic and potential energy.
- The REFPROP 10 library provides the streams' thermodynamic characteristics (Lemmon, Huber, and McLinden 2013), which is coupled with a MATLAB model that simulates the system.
- To prevent acid corrosion due to exhaust gas condensation, the lower limit of its temperature is set to 90°C (Hoang 2018).
- Finally, as an important factor, the maximum pinch point temperature difference in evaporators of the ORC and Kalina cycle is set to be 10°C. The concept of the Pinch point and its allocation was introduced and applied in the heat exchangers utilized in industries to maximize the heat recovery process (Linnhoff 1982). This concept is based on continuing the heat transfer process until its thermodynamically feasible energy targets within a process until the process is limited or pinched to its minimum temperature approach. However, even with a maximized heat recovery within a process, some residual heat will remain to be rejected by cooling water or air (Oluleye et al. 2016).

In Tables 2, 3 and 4 the assumptions required to perform the thermodynamic, techno-economic, and environmental analysis are referred to for each cycle.

3. Simulation

3.1. Thermodynamic analysis

To perform the thermodynamic analysis, each component is supposed to be a control volume. Based on the first law of thermodynamics, the corresponding mass and energy balances of each component are given in Equations (1-2).

$$\sum \dot{m}_{in} = \sum \dot{m}_{out} \quad (1)$$

$$\sum \dot{m}_{in} h_{in} + \dot{Q} = \sum \dot{m}_{out} h_{out} + \dot{W} \quad (2)$$

The ratio of total produced power to total heat input, which is computed as follows, is the energy efficiency, or efficiency of thermodynamics' first law, as specified in references:

$$\eta_I = \frac{\dot{W}_{net}}{\dot{Q}_{in}} \quad (3)$$

Table 2. Assumptions of Kalina cycle simulations.

| Kalina cycle | | | |
|--|------|---|-----|
| Exhaust gas inlet temperature (°C) | 180 | Turbine isentropic efficiency (%) | 85 |
| Exhaust gas outlet temperature (°C) | 90 | Pump isentropic efficiency (%) | 75 |
| Exhaust gas mass flow rate (kg.s ⁻¹) | 100 | Cooling water inlet temperature (°C) | 20 |
| Pinch point maximum temperature difference | 10 | Pinch point temperature difference of condenser | 5 |
| Flash Tank pressure (kPa) | 3000 | Cooling water pressure (kPa) | 100 |
| Flash tank inlet ammonia concentration (%) | 65 | Dead state temperature (°C) | 25 |
| Condenser outlet temperature (°C) | 32 | Dead state pressure (kPa) | 100 |

Table 3. Assumptions of ORC cycle simulations.

| ORC cycle | | | |
|--|---------------|---|-----|
| Exhaust gas inlet temperature (°C) | 180 | Turbine isentropic efficiency (%) | 85 |
| Exhaust gas outlet temperature (°C) | 90 | Pump isentropic efficiency (%) | 75 |
| Exhaust gas mass flow rate ($kg.s^{-1}$) | 100 | Cooling water inlet temperature (°C) | 20 |
| Pinch point maximum temperature difference of Evaporator | 10 | Pinch point temperature difference of condenser | 5 |
| Turbine inlet temperature (°C) | $T_{crit-10}$ | Dead state temperature (°C) | 25 |
| Condenser outlet temperature (°C) | 32 | Dead state pressure (kPa) | 100 |

Table 4. Assumptions of supercritical CO₂ cycle simulations.

| Supercritical CO ₂ cycle | | | |
|--|--------|---|-----|
| Exhaust gas inlet temperature (°C) | 500 | Turbine isentropic efficiency (%) | 85 |
| Exhaust gas outlet temperature (°C) | 300 | compressor isentropic efficiency (%) | 75 |
| Exhaust gas mass flow rate ($kg.s^{-1}$) | 100 | Cooling water inlet temperature (°C) | 20 |
| Turbine inlet temperature (°C) | 480 | Pinch point temperature difference of condenser | 5 |
| Compressor inlet temperature (°C) | 33 | Cooling water pressure (kPa) | 100 |
| Pressure ratio (-) | 200/77 | Dead state temperature (°C) | 25 |
| Dead state pressure (kPa) | 100 | | |

\dot{Q}_{in} in Eq. (3), indicates the heat provided by the exhaust gas and is equivalent to the enthalpy change of the heat source fluid across all cycles of the evaporator (Lecompte et al. 2014).

$$\dot{Q}_{in} = \dot{m}_{hs}(h_{hs,in} - h_{hs,out}) \quad (4)$$

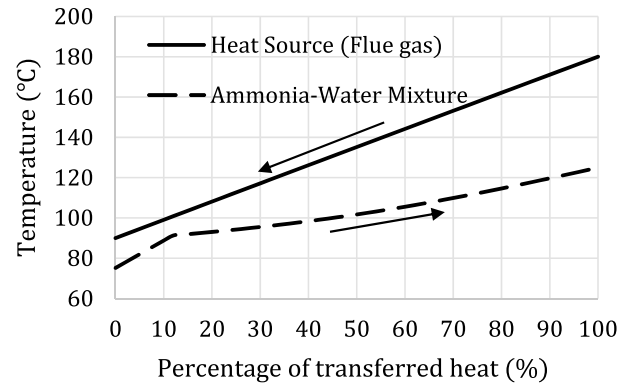
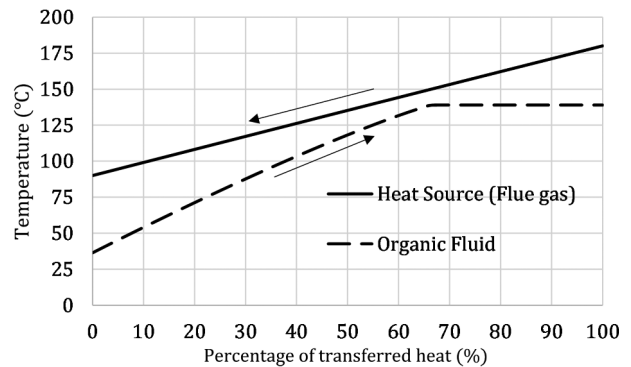
The net power production for each cycle, \dot{W}_{net} , is calculated using Eqs (5-7).

$$\dot{W}_{net} = \dot{W}_T - \dot{W}_P \quad (5)$$

$$\dot{W}_{Tur} = \dot{m}_{wf}(h_{Tur,in} - h_{Tur,out}) \quad (6)$$

$$\dot{W}_{Pu} = \dot{m}_{wf}(h_{Pu,in} - h_{Pu,out}) \quad (7)$$

The turbine inlet temperature in both ORC and Kalina cycles is adjusted based on the maximum temperature difference in their evaporators. For pure working fluids like refrigerants, the temperature increases or decreases in a linear trend, and their phase changes at a constant temperature. In contrast, for a mixture of water and ammonia, which is the working fluid of the Kalina cycle, the change in the temperature when the heat is transferred to or from the fluid, is not linear. Also, the phase-changing process does not happen isothermally. Hence, it is of high importance to find out the exact location of the pinch point in the heat exchangers that use water and ammonia mixtures. The most accurate method to locate the pinch point is to apply the discretization method, which means dividing each heat exchanger into finite sections (50 segments, in this study) and conducting the energy balance in each section. Hence, the pinch point is located, and violation from the maximum temperature difference will be checked. The following Figures 6, 7, and 8 present the temperature profile of Kalina, ORC, and super-critical CO₂ respectively. As shown in Figure 6, the evaporation process is a non-isothermal process, unlike the ORC evaporation process, plotted in Figure 7, mainly due to the nature of the ammonia-water mixture. While the super-critical CO₂ cycle has a non-isothermal heat transferring process because it is performed in a super-critical state, as represented in Figure 8.

**Figure 6.** Temperature profile (Temperature versus transferred heat) of evaporator in Kalina cycle.**Figure 7.** Temperature profile (Temperature versus transferred heat) of evaporator in ORC cycle.

3.2. Exergy efficiency

The exergy analysis, which determines how effective a system is at using its energy, will come after the thermodynamic first law (Adrian Bejan and Tsatsaronis 1995; Dincer and Rosen 2013). The terms kinetic, potential, chemical, and physical exergies are all included in the fluid flow exergy. The first two terms are not used in this report because it is assumed that they are generally understood. The following equations will be used to compute the system's exergy input (Mohammadkhani, Yari, and Ranjbar 2019):

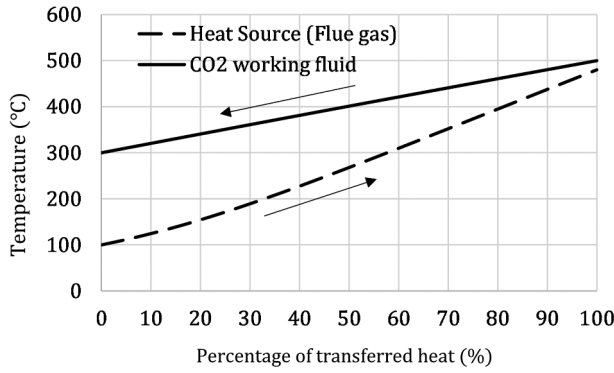


Figure 8. Temperature profile (Temperature versus transferred heat) of evaporator in sCO₂ cycle.

$$\dot{E}x_i = \dot{m}_i \times e_i \quad (8)$$

$$e_i^{ph} = (h_i - h_0) - T_0(s_i - s_0) \quad (9)$$

The state point in the figures and the conditions of the dead state are indicated, respectively, by the subscripts i and 0 .

Exergy efficiency or efficiency of thermodynamics 2nd law is defined as the exergy output in the evaporator divided by the exergy input to the system compared to the exergy flow of exhaust gas at the dead state, as shown in Eqs. (10)-(11).

$$\eta_{II} = \frac{\dot{W}_{net}}{\dot{E}x_{in}} \quad (10)$$

$$\dot{E}x_{in} = \dot{m}_{hs}(\dot{E}x_{hs,in} - \dot{E}x_0) \quad (11)$$

3.3. Economic analysis

In this study, as an economic analysis, a cost rate balance is applied to the overall system as follows. In Eq. (12), \dot{Z}_{total} and \dot{Z}_{Fuel} denote the total and fuel cost rates in \$/s, respectively:

Table 5. Cost functions of the components in the recovery cycles (Turton et al. 2001; Wang, Yang, and Xu 2021).

| components | correlation |
|--------------------------------|---|
| For all components except pump | $\dot{C}_{CI} = C_p F_{bm}$ (14) $\log C_p = K_1 + K_2 \log X + K_3 (\log X)^2$ $F_{bm} = B_1 + B_2 F_M$ |
| For pump | $\dot{C}_{CI} = C_p F_{bm}$ $\log C_p = K_1 + K_2 \log X + K_3 (\log X)^2$ $F_{bm} = B_1 + B_2 F_M F_p$ $\log F_p = C_1 + C_2 \log X + C_3 (\log X)^2$ |

Table 6. Coefficients of the components' Cost functions in the recovery cycles (Turton et al. 2001; Wang, Yang, and Xu 2021).

| Components | K_1 | K_2 | K_3 | C_1 | C_2 | C_3 | B_1 | B_2 | F_M | F_{bm} |
|-----------------|--------|--------|---------|---------|--------|---------|-------|-------|-------|----------|
| Heat exchangers | 4.3247 | -0.303 | 0.1634 | - | - | - | 1.63 | 1.66 | 1.38 | - |
| Turbine | 2.7051 | 1.4398 | -0.1776 | - | - | - | - | - | - | 6.2 |
| Compressor | 2.2898 | 1.3604 | -0.1027 | - | - | - | - | - | - | 5.8 |
| Pump | 3.8696 | 0.3161 | 0.1220 | -0.2454 | 0.2590 | -0.0136 | 1.89 | 1.35 | 1.38 | - |

$$\dot{Z}_{total} = \dot{Z}_{Fuel} + \dot{Z}_{env} + CEPCI \times \left[\sum_{i=1}^K (\dot{Z}_{CI} + \dot{Z}_{OM}) + BOS \right] \quad (12)$$

The capital investment cost rate (\dot{Z}_{CI}) for k th system component can be estimated as Table 5. \dot{Z}_{OM} are the cost rate associated with operation and maintenance for each component, often regarded as a percentage of the capital investment (\dot{Z}_{CI}). As seen, the costs associated with the separators, expansion valves, and mixing chambers are neglected due to their relatively negligible cost compared to the other components. The cost functions of the components and the associated coefficients are gathered in Tables 5 and 6 respectively.

For each component, the sum of capital cost and operating and maintenance cost are calculated using the following equation (Mosaffa, Mokarram, and Farshi 2017b):

$$\dot{Z}_{CI,K} = \frac{\dot{C}_{CI,K} \times CRF \times \emptyset}{t} \quad (13)$$

in which, \emptyset refers to the Maintenance factor, and t is the operational hours in a year.

A ratio used to determine the present value of a sequence of equal annual cash flows is called the capital recovery factor (CRF). Equation (14) can be used to calculate its value (Dincer and Rosen 2013).

$$CRF = \frac{i(i+1)^n}{(1+i)^n - 1} \quad (14)$$

Here, i is the interest rate and is assumed to be 8%, and n represents the project lifetime, which is considered 15 years (Georgousopoulos et al. 2021a).

In Table 5, X represents the power produces or consumes for turbine and pump, respectively, while for a heat exchanger means its heat transfer area. To calculate the heat transfer area, two methods are common: 1-Number of Transfer Units (NTU) method: is used to calculate heat transfer rate of heat exchangers, especially counter current ones, when there is insufficient information to calculate the log-mean temperature difference (LMTD). 2-LMTD method: can be used if the fluid inlet and outlet temperatures are obtained or can be with an energy balance. The heat transfer area is calculated based on the overall heat transfer coefficient U (Ahmed et al. 2018).

In this study, to calculate the heat transfer area for each evaporator, condenser, or other heat exchangers, the LMTD method through Equation (15) is used with applying constant overall heat transfer coefficient, for the sake of simplicity as performed in literature.

$$Q_{HX} = U_{HX} \times A_{HX} \times LMTD_{HX} \quad (15)$$

Where \dot{Q}_{HX} is the heat transfer rate in the heat exchanger in kW and U is the total heat transfer coefficient, A_{HX} is the heat transfer surface area in m^2 . The literature contains a number of sets of formulae for calculating the capital cost of the plant's components. A component's purchase price is significantly influenced by its size, heat transfer surface area, power output or consumption, manufacturing material, and type in relation to other types of that component. U for each heat exchanger of all three recovery cycles are referred in Table 7.

\dot{Z}_{Fuel} stands for the fuel cost to provide the thermal energy to run the systems. z_F is the unit cost of the exergy of the fuel in $$/kWh$, which is considered to be zero, in this study. As mentioned before, the fuel stream is the exhaust gas outlet from the glass furnace. Because no fuel is burnt to produce thermal energy as the hot source is the hot exhaust gas, it is reasonable to conclude that the exhaust gases emitted by the glass factory have no economic value when it enters the proposed system. Hence, for the proposed configuration of cycles, coupled with exhaust gas of a glass melting furnace as the heat source, z_F , and subsequently, \dot{Z}_F is considered zero.

$$\dot{Z}_{Fuel} = z_{Fuel} \dot{E}_{Fuel} \quad (16)$$

$$\dot{Z}_{env} = z_{CO_2} \times TEWI \quad (17)$$

$$TEWI = (GWP \times L_{annual} \times m_{charge} \times n) + GWP \times m_{charge} \times (1 - \beta_{recovery}) \quad (18)$$

\dot{Z}_{env} is the penalty cost of CO_2 emission where z_{CO_2} is the cost of CO_2 avoided. The TEWI which stands for Total Equivalent Warming Impact, can be evaluated as mentioned in Eq (18) where GWP is the global warming impact of the organic working fluid in kg CO_2 , which are specified in Table 8, L_{annual} is the annual leakage ratio of the organic fluid (kg) and $\beta_{recovery}$ is the percentage of the organic fluid recovery at the life end of

the system. The life of the system, n , is 15 years and m_{charge} is the amount of the organic fluid, which is injected into the system to make up the leaked fluid.

The penalty cost of CO_2 emissions is \dot{Z}_{env} , and the cost of CO_2 avoidance is \dot{Z}_{env} (Mosaffa et al. 2016). The term "TEWI," which stands for "Total Equivalent Warming Impact," can be calculated using Equation (18), where "GWP" refers for the organic working fluid's contribution to global warming in kilograms of carbon dioxide CO_2 as listed in Table 8 (Wijbenga et al. 2013). L_{annual} is the organic fluid's annual leakage ratio in kilograms, and $\beta_{recovery}$ is the system's lifetime organic fluid recovery as a percentage. The system has a 15-year lifespan, or n , and the amount of organic fluid called the m_{charge} that is pumped into it to replace the fluid that has leaked is called the "leaked fluid."

In this study, the balance of the system (BOS), which includes the cost of pipes, valves, the separator, and the operation and maintenance cost (\dot{Z}_{OM}), is taken into account as 20% and 6% of the updated capital cost investments of the components, such as $(CEPCI \times \sum \dot{Z}_{CI})$, respectively. Here, it is anticipated that the annual cost of operation and maintenance will equal 6% of the \dot{Z}_{CI} . As a result, the factor ϕ in Equation (13) is equal to 1.06 (Georgousopoulos et al. 2021a). Additionally, t is the system's 8000 yearly operating hours. By using the chemical engineering plant index (CEPCI), which is equivalent to 648.7/397, the capital cost is taken into account up until the year 2018 (Mosaffa et al. 2019).

ΔT_{ln} is the logarithmic mean temperature difference, and for a counterflow heat exchanger, it is calculated using the following equation.

$$\Delta T = \frac{(T_{h,in} - T_{c,out}) - (T_{h,out} - T_{c,in})}{\ln \left(\frac{T_{h,in} - T_{c,out}}{T_{h,out} - T_{c,in}} \right)} \quad (19)$$

Techno-economic analysis is performed by calculating some meaningful economic indicators. These parameters consider

Table 7. Overall heat transfer coefficients of heat exchangers (Mosaffa et al. 2017a, 2017b)-(Wang & Dai 2016)-(Zhang et al. 2018, 2019).

| Parameter | sign | cycle | Value | | | |
|-----------------------------------|------|-----------|------------|-----------|-----|-----------|
| | | | Evaporator | Condenser | IHE | Preheater |
| Overall Heat transfer coefficient | U | ORC cycle | 600 | 500 | 200 | - |
| | | s CO_2 | 1600 | 2000 | - | - |
| | | Kalina | 600 | 500 | 200 | 500 |

Table 8. Required coefficients in economic-environmental analysis.

| Parameter | sign | Value |
|--|--------------------|--------------------|
| Economical (Mokarram et al. 2020; Mosaffa et al. 2017a, 2017b; Noaman et al. 2019) | | |
| Annual interest rate | i | 0.08 |
| System lifetime | n | 15 |
| Maintenance factor | ϕ | 1.06 |
| Operational hours in a year | t | 8000 |
| Environmental (Garcia and Rosa 2019; Wijbenga et al. 2013) | | |
| cost of CO_2 avoided | c_{CO_2} | 87 |
| annual leakage ratio | L_{annual} | 0.02 |
| percentage of the organic fluid recovery | $\beta_{recovery}$ | 0.78 |
| Injected working fluid to the system | m_{charge} | 1.5 |
| GWP | GWP Ammonia-water | 5×10^{-4} |
| | GWP CO_2 | 1 |
| | GWP R245fa | 1030 |

the cost of power sold to the grid and the plant's annual profit. As a result, a techno-economic evaluation of the system is conducted here.

First, the Levelized cost of electricity (LCOE) will be calculated. Then, the techno-economic approach is applied via more insightful approaches, such as NPV (Net present value), IRR (internal rate of return), and PP (payback period). Applying this method of analyses can help to determine differences between the systems. To the current paper's economic analysis, it is assumed that no loan or subsidy has been obtained.

The levelized cost of electricity (LCOE) in dollars per kWh is proposed and calculated using Eq. (20) once the cost rates for capital expenditure, operation, and maintenance have been determined.

$$LCOE = \frac{\dot{Z}_{total}}{\dot{W}_{net}} \quad (20)$$

A common economic metric called net present value (NPV) depicts the current worth of an investment's potential net cash flow. It includes the annualized negative and positive cash flow cost calculations for the investment period. For a project to be considered acceptable, it must have a positive net present value (NPV), meaning that the cash inflow should be greater than the cash outflow.

The PEC in Eq. (22) includes only a part of the total capital investment (TCI), which means there will be additional costs, such as costs of additional miscellaneous equipment and costs related to the assembly of the cycles and its combination with the heat source as well as labor prices. A very common method to derive the TCI from the PEC is using a constant multiplication factor. In the literature, several such factors have been proposed (Georgousopoulos et al. 2021a). According to (Kolahi et al. 2016), the overall mentioned costs will be considered as 43% of the PEC:

$$TCI = 1.43 \times PEC \quad (21)$$

$$PEC_{total} = \sum_{i=1}^k \dot{C}_{CI,k} \quad (22)$$

$$NPV = -TCI + \sum_{t=1}^n \frac{AP}{(1+i)^t} \quad (23)$$

The lifespan of the plant and the nominal interest rate are represented by t and I , respectively. Using Equation (24) (Georgousopoulos et al. 2021a), AP is a calculation that represents the plant's annual profit. This study's running and maintenance costs are equivalent to the annual power sale minus ongoing annual costs.

$$AP = ((\dot{W}_{net} \times t \times C_{elec}) - \dot{Z}_{OM}) \quad (24)$$

C_{elec} is the unit price of electricity that is sold to the grid and is considered 0.1

The price per unit of electricity sold to the grid, or c_{elec} , is 0.1 \$/kWh (Kolahi et al. 2016). After determining the annual profit, it is possible to estimate other economic metrics, such as the (dynamic) payback time (PP), internal rate of return (IRR), and multiple of invested capital (MOIC). PP is the length of

time needed to recoup an investment's expenditure. In other words, it is the length of time needed for the NPV to progressively become zero. The return on investment is seen differently by IRR, on the other hand. IRR is the interest rate I at which the cash flow's NPV, or net present value, is equal to 0. MOIC is a different investment return factor from IRR in that it places more emphasis on "how much" than "when." It contrasts the initial investment with the present value of the projected profit flows during the project's lifetime. PP, IRR, and MOIC values can be calculated using Eqs. (25–27) (Georgousopoulos et al. 2021b; Kalogirou 2014). Since the value of IRR cannot be determined through simple calculations, the iterative technique is used.

$$PP = \frac{\ln(1 - \frac{TCI \times i}{AP})}{\ln(\frac{1}{1+i})} \quad (25)$$

$$0 = -TCI + \sum_{t=1}^n \frac{AP}{(1+IRR)^t} \quad (26)$$

$$MOIC = \sum_{t=1}^n \frac{(\frac{AP}{(1+i)^t})}{TCI} \quad (27)$$

4. Results and discussion

Three different cycles are studied and compared with the aim of waste heat recovery from glass-melting furnaces. Based on the available temperature, different type of recovery cycle is suggested. Both thermodynamic and techno-economic analyses have been performed to reveal the best possible option to recover the waste heat from exhaust gases of glass-melting furnaces. Also, the results of a parametric study are revealed to show the effect of key parameters in the thermodynamic and economic performance of three recovery cycles. ORC and Kalina cycles based on their natures will work with low-temperature sources, while a normal CO_2 cycle due to very low boiling temperature will not be able to run a power cycle. On the other hand, a low-temperature heat source cannot be utilized to work with the super-critical CO_2 cycle. A higher temperature source is suggested to match the sCO_2 cycle. Also, during the post-processes after melting glass, there are various levels with different temperatures. Therefore, different options are studied to have different solutions in different temperatures. The flue gas outlet from the melting furnace shows in the table. The working conditions are gathered in Tables 2, 3 and 4.

4.1. Comparison analysis

The final results of the thermodynamic and techno-economic analysis are summarized in Table 9. As shown, the supercritical CO_2 cycle has the highest power production up to 2.95 times versus Kalina's power production and 2 times higher than ORCs, as it is working with a higher temperature heat source. Though the first and second law efficiency is directly related to the power production, they are higher in the ORC cycle, which shows most of the thermal energy potential is still wasted in the

Table 9. Thermodynamic and economic results of waste heat recovery systems.

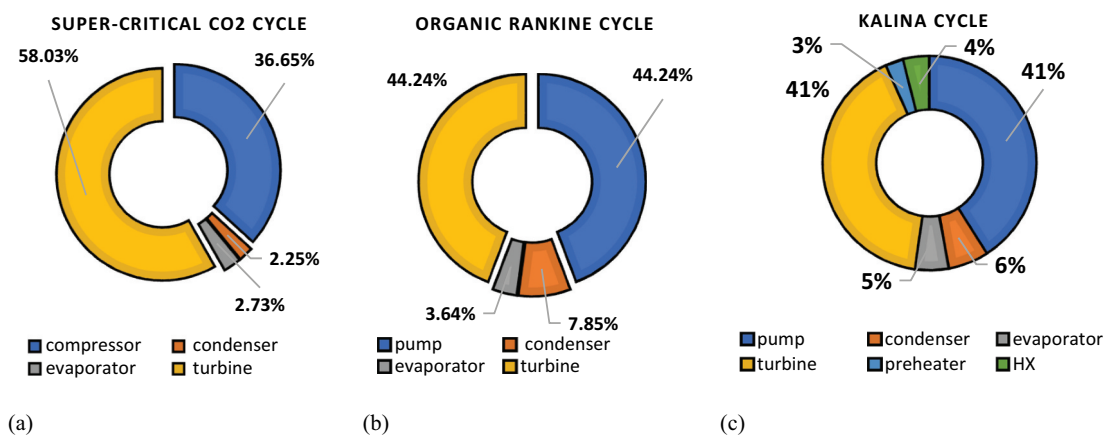
| Parameter | sCO ₂ | Kalina | ORC |
|--|------------------|--------------|--------------|
| \dot{W}_{net} (MW) | 3.1 | 1.06 | 1.54 |
| η_I (%) | 4.45 | 3.24 | 4.68 |
| η_{II} (%) | 13.7 | 25.99 | 37.53 |
| \dot{Z}_{total} (M\$. yr ⁻¹) | 0.7774 | 1.0690 | 0.8306 |
| LCOE (\$. kWh ⁻¹) | 0.0314 | 0.1254 | 0.0675 |
| AP (\$) | 2.12 e + 06 | 0.67 e + 06 | 2.084 e + 06 |
| PP (year) | 3.26 | 16.23 | 3.59 |
| IRR (%) | 35.97 | 9.33 | 32.98 |
| NPV (\$) | 1.49 e + 7 | 0.064 e + 07 | 1.41 e + 07 |
| MOIC (-) | 3.54 | 1.10 | 3.25 |

presumed supercritical CO₂ cycle. The comparison between the annual cost rates (\dot{z}_{tot}) of the cycles shows that the annual cost rate of the Kalina cycle is higher than those of the other ones (ORC and sCO₂) because the annual cost rate includes the capital cost of each component. Therefore, the components are the specifying factor on the final annual cost rate. As shown in Figure 9 turbines, pumps, and compressors are the components with higher capital costs in each heat recovery cycle. As shown in Figure 9(a), in the super-critical CO₂ cycle, the highest capital cost belongs to the turbine, compressor, evaporator, and condenser, respectively. While in Figure 9(b) for an ORC cycle, it is depicted that the turbine, pump, condenser, and evaporator have the highest capital cost. Also, for the Kalina cycle as drawn in Figure 9(c), after the turbine and pump, the highest capital cost belongs to the condenser, evaporator, internal heat exchanger, and preheater, respectively.

The LCOE as the other techno-economical parameter is calculated for the three waste heat recovery options. The results, as shown in Table 9, revealed that the Kalina cycle, the ORC, and sCO₂ have the most to the least LCOE based on the assigned working condition. LCOE varies with the capital investment cost of components as well as power production. Because the super-critical CO₂ cycle has the greatest power production, it has the lowest LCOE based on Equation (20). On the other hand, the Kalina cycle has the maximum capital cost of components, 1.37 and 1.28 times greater than those of sCO₂ and ORC, respectively. Therefore, it is logical to have the highest LCOE, based on the definition of LCOE in Equation (20). The ORC cycle has a medium LCOE among others, as it is neither as powerful as the sCO₂ cycle to produce power nor as expensive as the Kalina cycle because it is simpler and has fewer components than the Kalina cycle.

The next rows in Table 9 show other important techno-economic parameters named annual profit (AP), Payback Period (PP), Internal rate of return (IRR), Net present value (NPV), and multiple of invested capital (MOIC). As presented, the payback period for the Kalina cycle is the highest in terms of years, 4.97 and 4.52 times greater versus those of sCO₂ and ORC, because of the higher capital investment cost of its components, which means it takes more years to get back the capital investment price. Also, the annual profit for the Kalina cycle is the lowest due to its lowest power production compared to those of the sCO₂ and ORC cycles. sCO₂ has the highest annual profit, up to 3.16 and 1.01 times greater than those of Kalina and ORC, which means that PP for the Kalina cycle has the highest PP in between all three heat recovery options. While PP is the highest for the Kalina cycle, NPV has the least amount compared to those of other cycles, due to lower AP and higher capital investment cost, which leads to lower NPV for the Kalina cycle. The NPV of the sCO₂ cycle is 23 times greater versus that of Kalina, while it is only 1.05 times greater versus ORCs, which shows the approximate equality of the ORC cycle compared to the sCO₂. The same trend can be seen for the MOIC parameter. AP is the least for the Kalina cycle, while Capital investment cost, which means TCI, is the largest among those of other cycles. Thus, it ended up with the lowest amount of MOIC based on the MOIC correlation, Equation (27). MOIC of the sCO₂ cycle is 3.2 and 1.08 times greater compared to those of Kalina and ORC, respectively, which is another proof of ORC's priority when it is compared to two other options. Table 9 is visualized in Figure 10 to give a better vision of this comparison analysis.

Discussing the results based on the percentage difference, it would be interesting to see, the ORC cycle has only 8.3%, 5.3%,

**Figure 9.** Capital cost investment of components in the studied super-critical CO₂ cycle, ORC cycle, Kalina cycle.

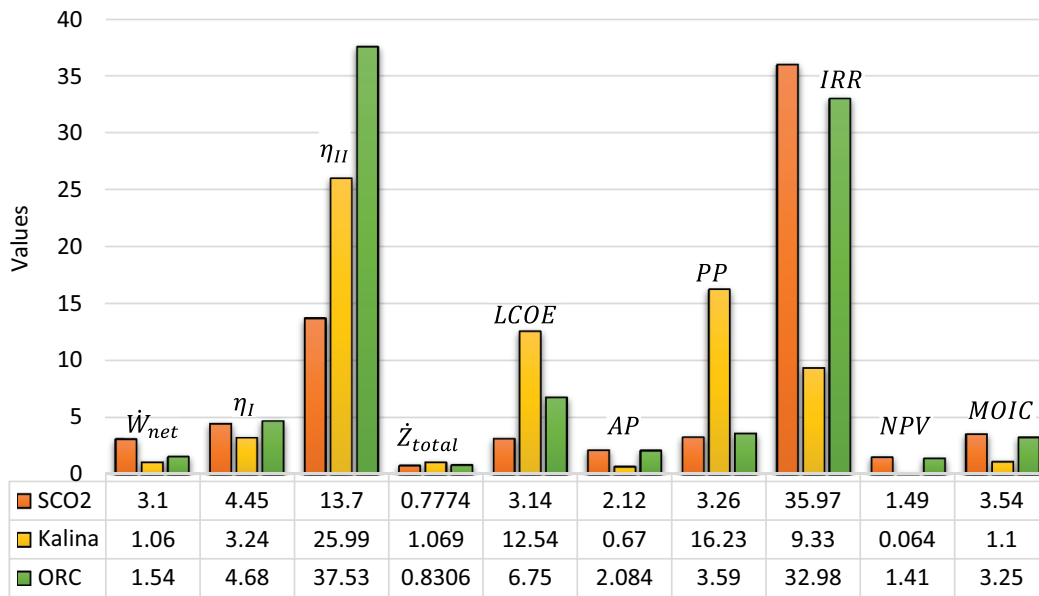


Figure 10. Comparison of calculated parameters in between three waste heat recovery cycles: sCO₂, Kalina, and ORC..

and 8.2% lower IRR, NPV, and MOIC compared to those of the sCO₂ cycle. Though ORC's period payback is 10% longer than that of sCO₂.

4.2. Parametric study

As mentioned before, a parametric study has been performed to understand the effects of the key parameters. For the ORC cycle, the effect of condenser temperature has been analyzed, while in the super-critical CO₂ cycle, the pressure ratio between turbine, and compressor and for the Kalina cycle the flash pressure are the key parameters that seem important to investigate.

Figure 11(a),(b) represents the thermodynamic and techno-economic parameters versus increasing condenser temperature. Increased condenser temperature leads to having higher saturated pressure in the condenser, which means higher enthalpy at the turbine outlet, lower enthalpy differences of the turbine, and lower turbine power production. As the power production goes lower, the first and second law efficiencies will have plummeted to 9.1% as shown in Figure 11(a). As Figure 11(b) shows MOIC, PP, and NPV decrease, while IRR increases. The reason is that lower power production means to have a lower total cost rate, lower PEC, and lower TCI as it is written in the related correlations, Equations (21–27).

Also, AP has a relation with the power production and the operating and maintenance costs based on Equation (24). Lower power production will decrease the operating and maintenance costs too because the operating and maintenance cost is a percentage of the total capital cost. Power production decreases and made decreases the operating and maintenance cost, but the latter has a negative sign in the correlation. Therefore, it will increase the AP, but the dominant parameter here is the decreasing power production, as AP goes lower (not shown in the figures).

On the other hand, NPV will be decreased. Lower TCI will lead to higher NPV due to the minus sign in Equation (23), while lower AP means lower NPV. The effect of AP dominates and leads to having lower NPV of up to 38.2%. Despite NPV,

IRR will be decreased up to 12%, as lower AP makes it lower, while lower TCI increases it. The effect of TCI has the greatest effect and makes IRR goes higher.

PP goes higher up to 17.2%, as it is related to TCI and AP, which both are decreasing. Inside the natural logarithm, TCI, and AP decrease in numerator and denominator, respectively, which leads to having lower PP because the lowered TCI has the most effect on the final behavior of PP.

MOIC goes lower with higher condenser temperature, because of the lower AP and TCI. Lowering TCI will increase MOIC as it is on the denominator but lowering AP will lower the MOIC. Because AP is the dominant parameter, MOIC finally will be decreased 9% with increasing condenser temperature.

Figure 12 presented the behavior of economic parameters versus the unit cost of electricity. As an important parameter, the unit cost of electricity is investigated in the parametric analysis, because the unit cost of electricity varies in different seasons and even from country to country and has a direct effect on the project profitability in different countries. Therefore, an analysis is performed to investigate the sensitivity of the economic parameters versus the unit cost of electricity.

NPV, shown on the second Y-axis of Figure 12, decreased up to 40 times with greater amounts of the unit cost of electricity, mainly due to higher annual profit as the effective parameter in its trend with varying pressure ratio. However, PP will be decreased up to 84% in the higher unit cost of electricity because increasing annual profit leads to lower PP based on Equation (25), while greater APs mean greater amounts of MOIC as well as IRR up to 3.4 times and 4.5 times, respectively.

As shown in Figure 13(a) power production, first and second law efficiencies go higher as the pressure ratio increases, because a higher-pressure ratio means to have more pressure drop in the turbine. This leads to a higher enthalpy difference in the turbine, which means higher power production.

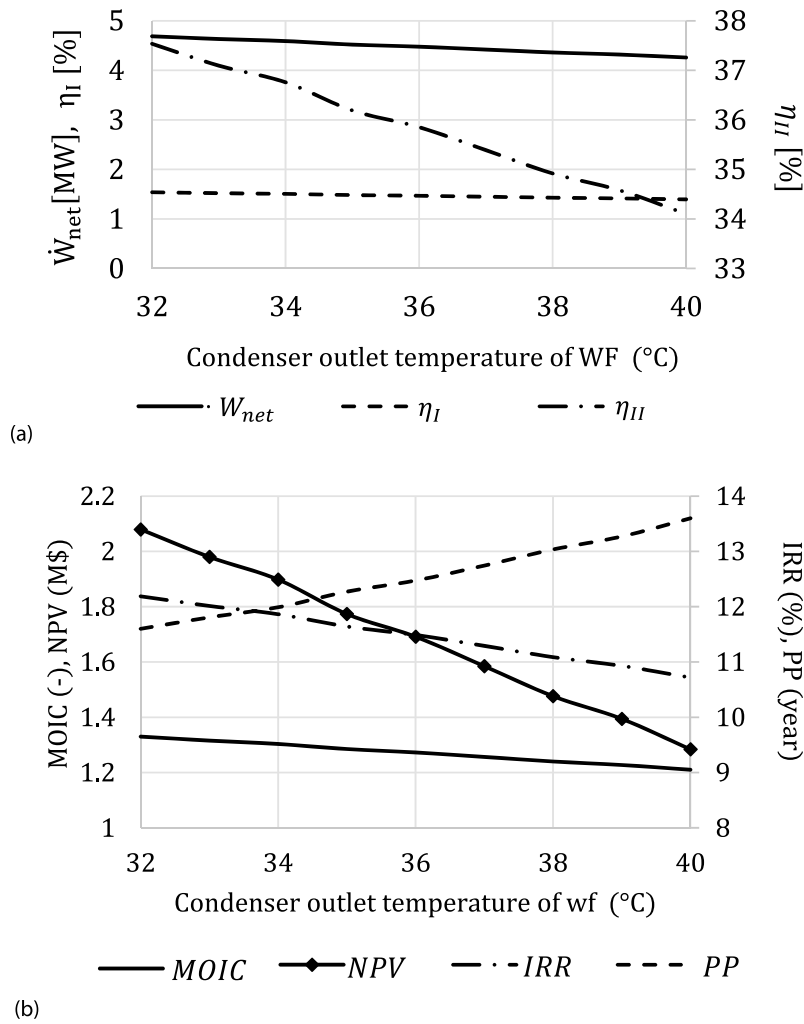


Figure 11. Variation of (a) thermodynamic parameters and (b) techno-economic parameters with increasing condenser temperature in ORC cycle.

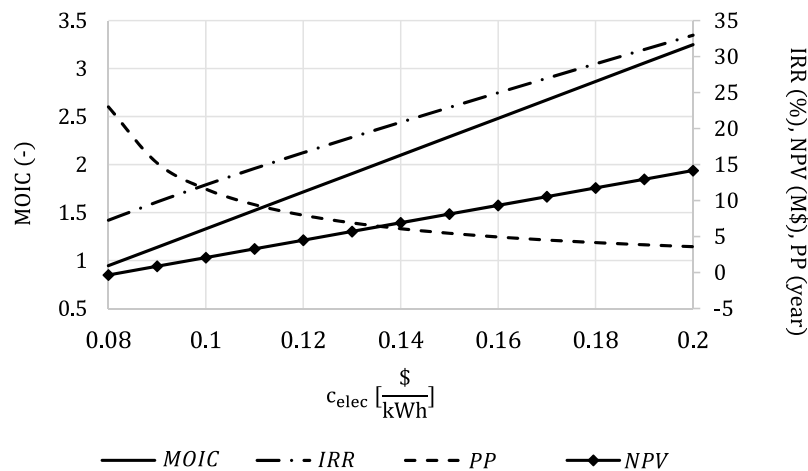


Figure 12. Variation of techno-economic parameters with increasing unit cost of electricity in ORC cycle.

In Figure 13(b) the variation of IRR, PP, NPV, and MOIC is drawn versus the pressure ratio of the supercritical CO₂ cycle. With increasing power production, AP, TCI, and PEC go higher. The PP goes lower at first and then goes higher as the pressure ratio increases. As the PP definition referred to in Equation (25) PP has a straightforward relationship with

the capital investment cost of components and therefore TCI, and an inverse relation with annual profit, AP. With an increased pressure ratio, both capital investment cost and annual profit will be increased. It means when PP goes lower, increasing annual profit dominates and makes PP lower. However, as the pressure ratio rises the increasing

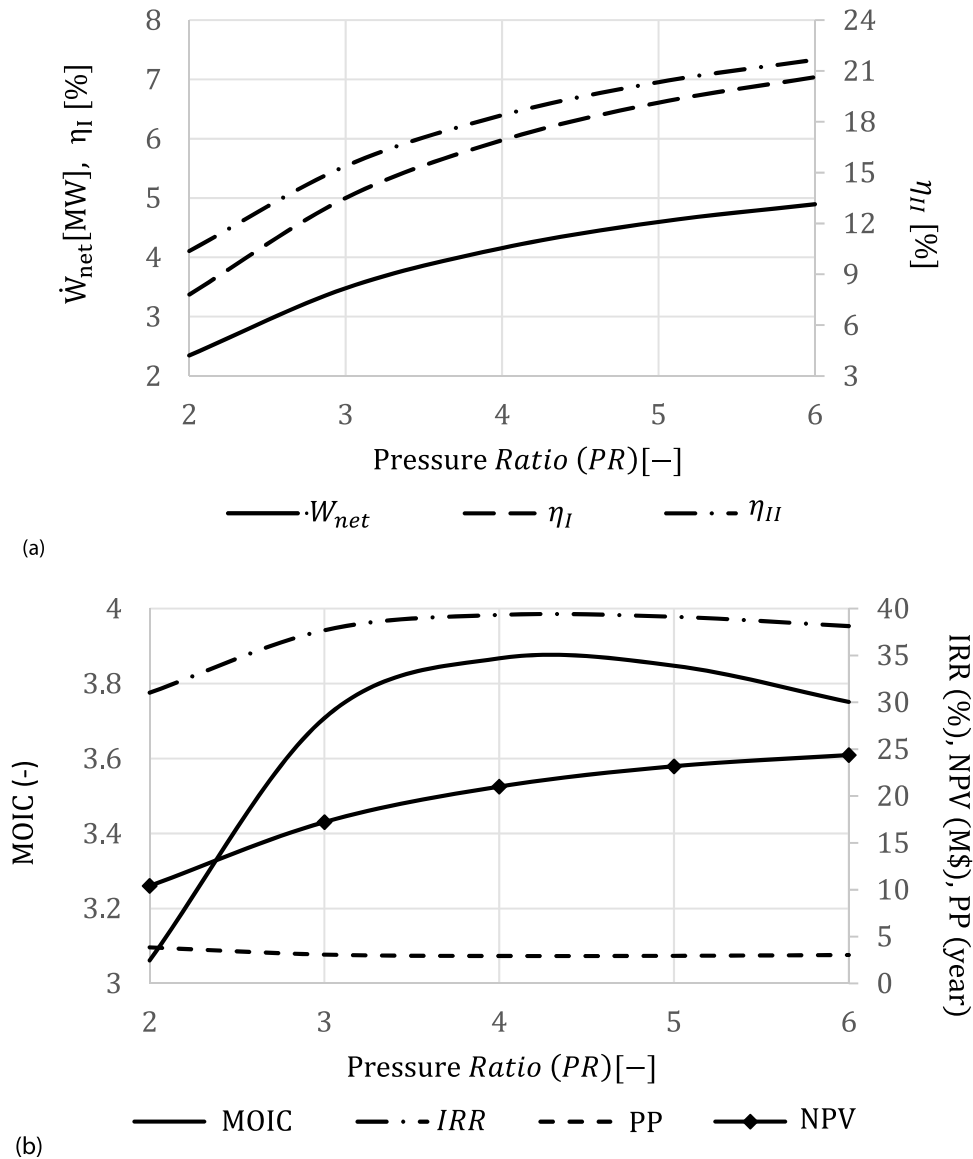


Figure 13. Variation of thermodynamic parameters and economical parameters with increasing the pressure ration in super-critical CO_2 cycle.

capital investment cost will cause PP to go higher gradually. On the other hand, MOIC shows an exactly reversed trend compared to PPs. MOIC increased first and then decreased. Because increasing annual profit dominates at lower pressure ratios, while capital investment cost will play the key role in higher pressure ratios. Also, it is shown that the NPV on the second y-axis of the plot in Figure 13(b) increases while varying the pressure ratio, due to being under the control of AP and TCI. AP is going higher as PR grows, as well as TCI. However, the changes due to increasing AP is more effective and lead to growing NPV with rising PR. The IRR as the other economic parameter goes higher at first, and then lower because of increasing AP and TCI as two effective parameters on its amount and behavior.

Figure 14 shows the effect of increasing flash pressure on thermodynamic and techno-economic parameters. Higher flash pressure means higher enthalpy at the turbine inlet state point, lower enthalpy difference of the turbine, and lower power production. On the other hand, increasing

pressure at the flash chamber will lead to a higher vapor mass flow rate. The increasing vapor mass flow rate is the prominent factor and leads to increased power production. Figure 14(b) shows the variation of techno-economic factors versus varying flash pressure. AP will be increased because of the higher power production and decreased due to total capital cost, but the final result is the increased annual profit.

Due to increasing power production, the total capital cost increased, which result in higher PEC and TCI. NPV has been affected by AP and TCI based on Equation (23). Increased AP and TCI lead to higher NPVs, which means AP is the dominant factor. The IRR goes higher as the flash pressure increases. Because TCI and AP go higher, increased TCI makes IRR lower, while higher AP means higher IRR. The result is a higher IRR. On the other hand, PP has been dropped. Higher TCI and AP will end up with lower PP, based on Equation (25). MOIC will be raised due to escalated AP and TCI. However, higher TCI decreases MOIC, while increasing AP means enhanced MOIC.

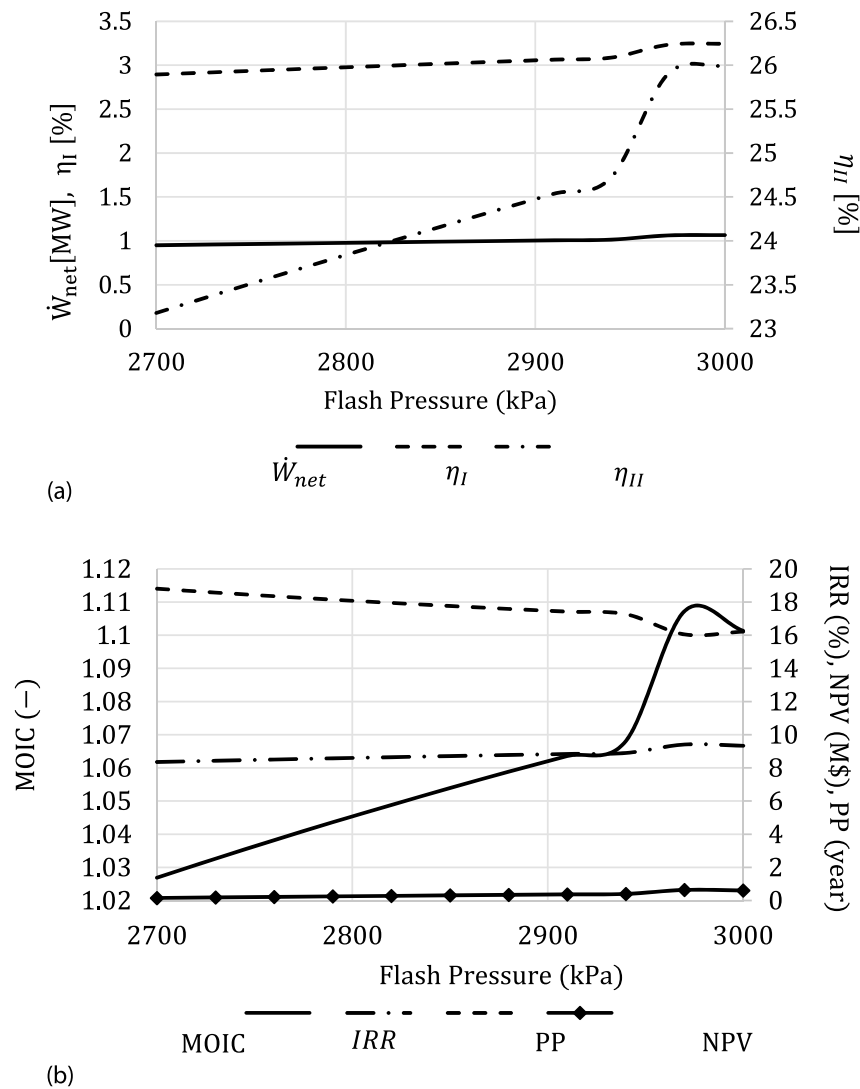


Figure 14. Variation of thermodynamic parameters and economical parameters with increasing the pressure ration in super-critical CO_2 cycle.

5. Conclusions

In this study, three different heat recovery cycles, ORC, $s\text{CO}_2$, and Kalina cycles, have been assessed to survey the possibility of recovering the waste heat from the exhaust gases of a real glass-melting furnace. The aim is to analyze and compare the waste heat recovery cycles for UK glass sectors. For the possible real temperatures of exhaust gas from UK glass melting furnaces, three basic recovery cycles analyzed to find the feasibility and possible risks based on techno-economic factors. A techno-economic analysis is applied to find out the best option between three different cycles to recover the waste heat. Two different plans are considered to work with low and high-temperature heat sources. Super-critical CO_2 cycle is linked to a high-temperature source, while the ORC and Kalina cycles are satisfactory to work with low-temperature waste heat. LCOE, IRR, PP, and MOIC are four parameters calculated in this report. The results show that capital investment costs of the turbines, pumps, and compressor have the greatest shares in three cycles. Also, based on the parameters calculated, it is presented that the best option will be the ORC cycle for low-temperature waste heat, though $s\text{CO}_2$ which is

the only option surveyed for high temperature, has the largest power production due to the higher temperature exhaust gases. The result showed that $s\text{CO}_2$ has the greatest power production, IRR, NPV and MOIC equal to 3.1 MW, 35.97%, $1.49\text{e} + 7$ \$, and 3.54, respectively. Though ORC's amounts are not that faraway from those of $s\text{CO}_2$. On the other hand, the AP and PP of the ORC cycle are the greatest, with the amounts of $2.12\text{e} + 6$ \$ and 3.59 years, while Kalina cycle has the highest costs based on total cost and LCOE equal to 1.069 ($\text{M}\$. \text{yr}^{-1}$) and 0.1254 ($\$. \text{kWh}^{-1}$). The only advantage of supercritical CO_2 is its power production, which is 2.9 times greater than Kalina's and 2 times greater than ORCs. Even the first law efficiency of ORC is 95% of the $s\text{CO}_2$'s and the second law efficiency of ORC is 2.5 times greater than $s\text{CO}_2$'s. Speaking economically, the annual profit of $s\text{CO}_2$ (AP), IRR, NPV, and MOIC of the ORC cycle are only 1.01, 1.09, 1.05, and 1.09 times greater than those of ORC, respectively. Therefore, ORC has all advantages except the higher power production, compared to $s\text{CO}_2$. Though, it cannot be used for higher temperatures, unless changing the working conditions to work within supercritical regions.

Nomenclature

| | |
|-----------------|--|
| A | area (m ²) |
| AP | annual profit |
| \dot{Z} | cost rate (\$ s ⁻¹) |
| \dot{C}_{CI} | capital investment cost rate |
| c_{elec} | Unit price of electricity |
| CRF | capital recovery factor |
| comp | compressor |
| cond | condenser |
| (D)PP | (Dynamic) period payback |
| e^0 | standard chemical exergy (kJ kmol ⁻¹ K ⁻¹) |
| e_{ph} | Physical exergy flow |
| e_{ch} | Chemical exergy flow |
| \dot{E} | exergy rate (kW) |
| EXP | Expansion valve |
| FT | Flash tank |
| h | specific enthalpy (kJ kg ⁻¹) |
| i | Nominal interest rate |
| IRR | Internal rate of return (%) |
| $K_i i = 1 : 3$ | constant coefficients of heat exchanger cost functions |
| LCOE | Levelized cost of energy (\$/Kwh ⁻¹) |
| \dot{m} | mass flow rate (kg s ⁻¹) |
| MOIC | multiple of investment capital (-) |
| MW | molecular weight (kg kmol ⁻¹) |
| MiX | mixing chamber |
| n | system lifetime (year) |
| NPV | net present value (\$) |
| ORC | Organic Rankine cycle |
| PEC | purchased equipment cost |
| PR | Pressure ratio |
| Pu | pump |
| Q | heat rate (kW) |
| Re | recuperator |
| s | specific entropy (kJ kg ⁻¹ K ⁻¹) |
| T | temperature (K) |
| t | operational hours in a year |
| Tur | turbine |
| TCI | Total capital investment |
| ΔT_{ln} | logarithmic mean temperature difference (K) |
| U | overall heat transfer coefficient (W m ⁻² K ⁻¹) |
| \dot{W} | power (kW) |
| Greek symbols | |
| ϕ | maintenance factor |
| ΔT_{ln} | logarithmic mean temperature difference |
| η | Efficiency (%) |
| η_{is} | isentropic efficiency (%) |
| Subscripts | |
| 0 | ambient |
| 1, 2, 3, ... | State points |
| in | inlet |
| HX | Heat exchanger |
| O&M | Operating and maintenance (cost) |
| out | outlet |
| P | pump |
| tot | total |

Disclosure statement

No potential conflict of interest was reported by the authors.

Funding

This work was supported by the Innovate UK under Grant 10018130

References

- Adrian Bejan, M. J. M., and G. Tsatsaronis. 1995. *Thermal design and optimization*. Wiley. 978-0-471-58467-4.
- Ahmed, A., K. K. Esmaeil, M. A. Irfan, and F. A. Al-Mufadi. 2018. Design methodology of organic Rankine cycle for waste heat recovery in cement plants. *Applied Thermal Engineering* 129:421–30. Jan. doi: 10.1016/j.applthermaleng.2017.10.019.
- Baldi, F., and C. Gabrieli. 2015. A feasibility analysis of waste heat recovery systems for marine applications. *Energy* 80:654–65. doi:10.1016/j.energy.2014.12.020.
- Bause, T., F. Campana, L. Filippini, A. Foresti, and N. Monti. 2014. Cogeneration with ORC at Elbe-Stahlwerke Feralpi EAF Shop. In Proceedings of the Iron & Steel Technology Conference and Exposition, Indianapolis, USA, 5-8 May, 2014. <https://www.aist.org/conference-expositions/aistech/past-events/aistech-2014/>
- Brückner, S., S. Liu, L. Miró, M. Radspieler, L. F. Cabeza, and E. Lävemann. 2015. Industrial waste heat recovery technologies: An economic analysis of heat transformation technologies. *Applied Energy* 151:157–67. doi:10.1016/j.apenergy.2015.01.147.
- Dalton, D., British Glass CEO. 2019. Glass sector Net zero strategy 2050. <https://www.britglass.org.uk/sites/default/files/British%20Glass%20-%20Net%20Zero%20Strategy.pdf>
- Dincer, I., and M. A. Rosen. 2013. *Exergy: Energy, Environment and Sustainable Development*. 2nd ed. 9780080970905.
- Dolianitis, I., D. Giannakopoulos, C. Stavroula Hatzilau, S. Karellas, E. Kakaras, E. Nikolova, G. Skarpetis, N. Christodoulou, N. Giannoulas, and T. Zitounis. 2016. Waste heat recovery at the glass industry with the intervention of batch and cullet preheating. *Thermal Science* 20 (4):1245–58. doi:10.2298/TSCI151127079D.
- The European Container Glass Federation. Waste heat recovery technologies largely used in the European container glass industry to optimize energy consumption and reduce co2 emissions. <https://feve.org/case-study/waste-heat-recovery-technologies-largely-used-in-the-european-container-glass-industry-to-optimize-energy-consumption-and-reduce-co2-emissions/>
- Garcia, J. M., and A. Rosa. 2019. Theoretical study of an intermittent water-ammonia absorption solar system for small power ice production. *Sustainability (Switzerland)* 11 (12):3346. doi:10.3390/SU11123346.
- Georgousopoulos, S., K. Braimakis, D. Grimekis, and S. Karellas. 2021a. Thermodynamic and techno-economic assessment of pure and zeotropic fluid ORCs for waste heat recovery in a biomass IGCC plant. *Applied Thermal Engineering* 183:116202. doi:10.1016/j.applthermaleng.2020.116202.
- Georgousopoulos, S., K. Braimakis, D. Grimekis, and S. Karellas. 2021b. Thermodynamic and techno-economic assessment of pure and zeotropic fluid ORCs for waste heat recovery in a biomass IGCC plant. *Applied Thermal Engineering* 183:116202. Jan. doi: 10.1016/j.applthermaleng.2020.116202.
- British Glass. 2017. Glass sector joint industry-government industrial decarbonisation and energy efficiency roadmap action plan. https://assets.publishing.service.gov.uk/government/uploads/system/uploads/attachment_data/file/652080/glass-decarbonisation-action-plan.pdf
- Glass Alliance Europe, “Main glass sectors,” 2022. <https://www.glassallianceeurope.eu/en/main-glass-sectors>
- Hassani Mokarram, N., and A. H. Mosaffa. 2020. Investigation of the thermoeconomic improvement of integrating enhanced geothermal single flash with transcritical organic rankine cycle. *Energy Conversion and Management* 213 (April):112831. doi:10.1016/j.enconman.2020.112831.
- Hedin, N., L. Andersson, L. Bergström, and J. Yan. 2013. Adsorbents for the post-combustion capture of CO2 using rapid temperature swing or vacuum swing adsorption. *Applied Energy* 104:418–33. doi:10.1016/j.apenergy.2012.11.034.

- Hoang, A. T. 2018. Waste heat recovery from diesel engines based on organic rankine cycle. *Applied Energy* 231:138–66. Dec. doi: 10.1016/j.apenergy.2018.09.022.
- Ipakchi, O., A. H. Mosaffa, L. Garousi Farshi. 2019. Ejector based CO₂ transcritical combined cooling and power system utilizing waste heat recovery: A thermoeconomic assessment. *Energy Conversion and Management* 186 (January):462–72. doi:10.1016/j.enconman.2019.03.009.
- Kalina, A. I., H. M. Leibowitz, V. President, and A. Systems. 1988. The design of a 3mw kalina cycle experimental Plant. Gas Turbine and Aeroengine Congress, Amsterdam, The Netherlands, The American Society Of Mechanical Engineers.
- Kalogirou, S. A. 2014. *Solar energy engineering: processes and systems*. ed. Second Edition. Elsevier Inc. doi:10.1016/C2011-0-07038-2.
- Kolahi, M., M. Yari, S. M. S. Mahmoudi, and F. Mohammadkhani. 2016. Thermodynamic and economic performance improvement of ORCs through using zeotropic mixtures: Case of waste heat recovery in an offshore platform. *Case Studies in Thermal Engineering* 8:51–70. doi:10.1016/j.csite.2016.05.001.
- Larjola, J. 1995. Electricity from industrial waste heat using high-speed organic Rankine cycle (ORC). *International Journal of Production Economics* 41 (1–3):227–35. doi:10.1016/0925-5273(94)00098-0.
- Lecompte, S., B. Ameel, D. Ziviani, M. Van Den Broek, and M. De Paepe. 2014. Exergy analysis of zeotropic mixtures as working fluids in organic rankine cycles. *Energy Conversion and Management* 85:727–39. Sep. doi: 10.1016/j.enconman.2014.02.028.
- Lecompte, S., O. Oyewunmi, C. Markides, M. Lazova, A. Kaya, M. van den Broek, and M. De Paepe. 2017. Case study of an Organic Rankine cycle (ORC) for waste heat recovery from an electric arc furnace (EAF). *Energies (Basel)* 10 (5):649. doi:10.3390/en10050649.
- Lemmon, E., M. Huber, and M. McLinden. national institute of standards and technology (NIST). 2013. Natl Std. Ref. Data Series (NIST NSRDS). <https://www.nist.gov/publications/nist-standard-reference-database-23-reference-fluid-thermodynamic-and-transport>
- Linnhoff, B. 1982. The pinch design method for heat exchanger networks. *Chemical Engineering Science*. doi:10.1016/0009-2509(83)80185-7.
- Li, C., and H. Wang. 2016. Power cycles for waste heat recovery from medium to high temperature flue gas sources – from a view of thermodynamic optimization. *Applied Energy* 180:707–21. Oct. doi: 10.1016/j.apenergy.2016.08.007.
- Modi, A. DTU, Denmark. 2015. Numerical evaluation of the Kalina cycle for concentrating solar power plants. https://backend.orbit.dtu.dk/ws/portalfiles/portal/118944026/S188_Anish_Modi_FINAL_Web.pdf
- Mohammadkhani, F., M. Yari, and F. Ranjbar. 2019. A zero-dimensional model for simulation of a diesel engine and exergoeconomic analysis of waste heat recovery from its exhaust and coolant employing a high-temperature Kalina cycle. *Energy Conversion and Management* 198 (May):111782. doi:10.1016/j.enconman.2019.111782.
- Mokarram, N. H., and A. H. Mosaffa. 2018. A comparative study and optimization of enhanced integrated geothermal flash and Kalina cycles: A thermoeconomic assessment. *Energy* 162:111–25. Nov. doi: 10.1016/j.energy.2018.08.041.
- Mosaffa, A. H., L. G. Farshi, C. A. Infante Ferreira, and M. A. Rosen. 2016. Exergoeconomic and environmental analyses of CO₂/NH₃ cascade refrigeration systems equipped with different types of flash tank intercoolers. *Energy Conversion and Management* 117:442–53. Jun. doi: 10.1016/j.enconman.2016.03.053.
- Mosaffa, A. H., N. H. Mokarram, and L. G. Farshi. 2017a. Thermoeconomic analysis of a new combination of ammonia/water power generation cycle with GT-MHR cycle and LNG cryogenic exergy. *Applied Thermal Engineering* 124:1343–53. doi:10.1016/j.applthermaleng.2017.06.126.
- Mosaffa, A. H., N. H. Mokarram, and L. G. Farshi. 2017b. Thermoeconomic analysis of combined different ORCs geothermal power plants and LNG cold energy. *Geothermics* 65:113–25. doi:10.1016/j.geothermics.2016.09.004.
- Musiał, A. M., Ł. Antczak, Ł. Jędrzejewski, and P. Klonowicz. 2021. Analysis of the use of waste heat from a glass melting furnace for electricity production in the organic Rankine cycle system. *Archives of Thermodynamics* 42 (1):15–33. doi:10.24425/ather.2021.136945.
- Nascimento, M. L. F. 2014. Brief history of the flat glass patent - Sixty years of the float process. *World Patent Information* 38:50–56. doi:10.1016/j.wpi.2014.04.006.
- Noaman, M., G. Saade, T. Morosuk, and G. Tsatsaronis. 2019. Exergoeconomic analysis applied to supercritical CO₂ power systems. *Energy* 183:756–65. Sep. doi: 10.1016/j.energy.2019.06.161.
- Oluleye, G., M. Jobson, R. Smith, and S. J. Perry. 2016. Evaluating the potential of process sites for waste heat recovery. *Applied Energy* 161:627–46. Jan. doi: 10.1016/j.apenergy.2015.07.011.
- Omar, A., M. Saghafifar, K. Mohammadi, A. Alashkar, and M. Gadalla. 2019. A review of unconventional bottoming cycles for waste heat recovery: Part II – Applications. *Energy Conversion and Management* 180:559–83. doi:10.1016/j.enconman.2018.10.088. Elsevier Ltd.
- Philibert, C. Environment Directorate, International Energy Agency IEA, Organisation for Economic Co-operation and Development OECD, Paris (France). 2007. Technology penetration and capital stock turnover. Lessons from IEA scenario analysis. https://www.osti.gov/etde_web/biblio/20962174
- Polytechnic, K. 1998. 98/01752 a review of organic Rankine cycles (ORCs) for the recovery of low-grade waste heat. *Fuel and Energy Abstracts* 39 (2):151. doi:10.1016/s0140-6701(98)97894-8.
- Quoilin, S., M. Van Den Broek, S. Declaye, P. Dewallef, and V. Lemort. 2013. Techno-economic survey of organic rankine cycle (ORC) systems. *Renewable and Sustainable Energy Reviews* 22:168–86. doi:10.1016/j.rser.2013.01.028.
- Shu, G., Y. Liang, H. Wei, H. Tian, J. Zhao, and L. Liu. 2013. A review of waste heat recovery on two-stroke IC engine aboard ships. *Renewable and Sustainable Energy Reviews* 19:385–401. doi:10.1016/j.rser.2012.11.034.
- Sovacool, B. K., M. Bazilian, S. Griffiths, J. Kim, A. Foley, and D. Rooney. 2020. Decarbonizing the food and beverages industry: A critical and systematic review of developments, sociotechnical systems and policy options. *Renewable and Sustainable Energy Reviews* 143 (September):110856. 2021. doi:10.1016/j.rser.2021.110856.
- Sovacool, B. K., S. Griffiths, J. Kim, and M. Bazilian. 2021. Climate change and industrial F-gases: A critical and systematic review of developments, sociotechnical systems and policy options for reducing synthetic greenhouse gas emissions. *Renewable and Sustainable Energy Reviews*, 141 (August):110759. 2020. doi:10.1016/j.rser.2021.110759.
- Tartière, T., and M. Astolfi. 2017. A world overview of the organic Rankine Cycle Market. *Energy Procedia* 129:2–9. doi:10.1016/j.egypro.2017.09.159.
- Turton, R., R. C. Bailie, W. B. Whiting, J. A. Shaeiwitz, and D. Bhattacharyya. 2001. *Analysis, Synthesis, and Design of Chemical Processes*. 40 (6). doi: 10.1002/1521-3773(20010316)40:6<9823::AID-ANIE98233.3.CO;2-C.
- Valenti, G., A. Valenti, and S. Staboli. 2019. Proposal of a thermally-driven air compressor for waste heat recovery. *Energy Conversion and Management* 196:1113–25. Sep. doi: 10.1016/j.enconman.2019.06.072.
- Wang, X., and Y. Dai. 2016. Exergoeconomic analysis of utilizing the transcritical CO₂ cycle and the ORC for a recompression supercritical CO₂ cycle waste heat recovery: A comparative study. *Applied Energy* 170:193–207. May. doi: 10.1016/j.apenergy.2016.02.112.
- Wang, J., Y. Dai, and L. Gao. 2009. Exergy analyses and parametric optimizations for different cogeneration power plants in cement industry. *Applied Energy* 86 (6):941–48. doi:10.1016/j.apenergy.2008.09.001.
- Wang, Y., H. Yang, and K. Xu. 2021. Thermo-economic investigation and optimization of parallel double-evaporator organic Rankine & Kalina cycles driven by the waste heat of an industrial roller kiln: A comparative study. *Energy Reports* 7:2276–93. doi:10.1016/j.egy.2021.04.018.
- Wijbenga, H., M. V. D. Hoff, M. Janssen, and C. A. I. Ferreira. 2013. Life cycle performance of refrigeration systems in the Dutch food

- and beverages sector. 4th IIR Conference on Thermophysical Properties and Transfer Processes of Refrigerants, Delft, Netherlands.
- Yu, S. C., L. Chen, Y. Zhao, H. X. Li, and X. R. Zhang. 2015. A brief review study of various thermodynamic cycles for high temperature power generation systems. *Energy Conversion and Management* 94:68–83. doi:10.1016/j.enconman.2015.01.034.
- Zhang, Q., Z. Luo, Y. Zhao, and R. Cao. 2019. Performance assessment and multi-objective optimization of a novel transcritical CO₂ trigeneration system for a low-grade heat resource. *Energy Conversion and Management* 204 (November):112281. 2020. doi:10.1016/j.enconman.2019.112281.
- Zhang, Q., R. M. Ogren, and S. C. Kong. 2018. Thermo-economic analysis and multi-objective optimization of a novel waste heat recovery system with a transcritical CO₂ cycle for offshore gas turbine application. *Energy Conversion and Management* 172 (Sep):212–27. doi:10.1016/j.enconman.2018.07.019.
- Zier, M., P. Stenzel, L. Kotzur, and D. Stolten. A review of decarbonization options for the glass industry. *Energy Conversion and Management* 10:100083. 10.1016/j.ecmx.2021.100083. Elsevier Ltd. Jun. 1, 2021